Journal of Macromolecular Science, Part A
Publication details, including instructions for authors and subscription information:
http://www.informaworld.com/smpp/title~content=t713597274

Thermo-mechanical Properties of PEO-PU/PAN Semi-Interpenetrating Polymer Networks and their $LiClO_4$ Salt-Complexes

Pratyay Basak[a]; Sunkara V. Manorama[a]
[a] Materials Science Group, Inorganic and Physical Chemistry Division, Indian Institute of Chemical Technology, Hyderabad, India

To cite this Article Basak, Pratyay and Manorama, Sunkara V.(2006) 'Thermo-mechanical Properties of PEO-PU/PAN Semi-Interpenetrating Polymer Networks and their $LiClO_4$ Salt-Complexes', Journal of Macromolecular Science, Part A, 43: 2, 369 — 382
To link to this Article: DOI: 10.1080/10601320500437292
URL: http://dx.doi.org/10.1080/10601320500437292

Journal of Macromolecular Science®, Part A: Pure and Applied Chemistry, 43:369–382, 2006

ISSN 1060-1325 print/1520-5738 online
DOI: 10.1080/10601320500437292

Thermo-mechanical Properties of PEO-PU/PAN Semi-Interpenetrating Polymer Networks and their $LiClO_4$ Salt-Complexes†

PRATYAY BASAK AND SUNKARA V. MANORAMA

Materials Science Group, Inorganic and Physical Chemistry Division, Indian Institute of Chemical Technology, Hyderabad, India

This paper is an investigation on the thermo-mechanical properties of a new class of materials, which holds promise for its potential use as solid polymer electrolytes, i.e., SPE material. A series of poly(ethylene oxide)-polyurethane/poly(acrylonitrile) (PEO-PU/PAN) semi-IPNs, along with their $LiClO_4$ salt complexes, were characterized for their thermal, mechanical and dimensional stability using DSC, TG-DTA, UTM and DMTA. The glass transition temperature (T_g) of both the undoped and doped semi-IPNs, obtained by DSC, remained well below room temperature ($\sim -50^\circ C$ to $-35^\circ C$), satisfying one of the essential requirements to serve as a SPE host matrix. The crystallization process in the PEO segments of the PEO-PU/PAN semi-IPNs was prevented at higher salt concentrations, which is attributed to the Li^+ ion mediated pseudo-crosslinks. Good thermal stability of the semi-IPNs was evident from the degradation onset temperature ($T_0 \sim 240^\circ C$) with a three-stage degradation process, which is independent of the PAN content as observed from differential thermogravimetric studies. The incorporation of PAN in the PEO-PU networks results in improved mechanical properties, such as tensile strength and modulus while retaining the flexibility of the semi-IPNs. The peak temperatures and storage modulus obtained from DMTA correlates well with the observations of DSC and tensile measurements.

Keywords interpenetrating polymer networks, solid polymer electrolytes, poly(ethylene oxide), poly(acrylonitrile)

Introduction

Polymer-salt complexes have attracted a lot of attention for the last few decades, ever since Wright (1) and Armand (2) put forward the concept for their use as solid polymer electrolytes (SPEs). Thereafter, several studies have been directed towards identifying polymers suitable as host matrices, their electrical and electrochemical behavior and the mode of ion-conduction in such systems (3–10). A conductivity threshold value of approximately 10^{-5} Scm^{-1} and an electrochemical stability window of ~ 4 V, has been

Received January 2005; Accepted June 2005.
†IICT Communication No.: 0407019.
Address correspondence to Sunkara V. Manorama, Materials Science Group, Inorganic and Physical Chemistry Division, Indian Institute of Chemical Technology, Hyderabad 500 007, India; Tel.: +9140-27160123, Extn: 2386; Fax: +9140-27160921; E-mail: manorama@iict.res.in

used as the criterion for possible application purposes (3, 4). Two aspects in particular govern the magnitude of conductivity in SPEs, the degree of crystallinity and the salt concentration. Ionic conductivity in these highly disordered systems occurs primarily in the amorphous regions and is associated with both charge migration of ions between coordination sites (ionic hopping) and the polymeric chain segmental motions (micro-Brownian motions). The dynamic bond percolation theory developed by Ratner et al. explains the charge migration in such systems in terms of renewal of hopping probabilities (5, 9).

Among several prospective hosts, poly(ethylene oxide) (PEO) (1, 3–6, 11–13) and poly(acrylonitrile) (PAN) (14–18) are the ones most studied. However, several bottlenecks still remain in bringing this idea to complete fruition. Apart from the inherent heterogeneity of the polymer-salt matrices, the thermal and mechanical stabilities necessary for these materials to be used in devices at ambient conditions are of primary concerns and are still a challenge to be addressed. Among all the techniques suggested to improve the matrix property, like blending (19, 20), co-polymerization (21–23), grafting (24, 25) and network formation (26–28), the last modification has been predicted to be the most viable alternative.

From this perspective, interpenetrating polymer networks (IPNs) can be thought to be advantageous in several respects, especially where dimensional, thermal and mechanical stability along with homogeneity and lower degree of crystallinity of the polymer matrix are the prerequisites. However, the literature survey reveals that though IPNs of several polymer combinations have been studied in great detail very little attention has been directed towards their end use as SPEs.

In an effort to demonstrate the feasibility of IPNs as host matrices for SPEs, a model system of PEO-PU/PAN semi-IPNs and their $LiClO_4$ salt-complexes have been synthesized. Studies on their electrical behavior and their dependence on the physical properties have been reported elsewhere (29). With varying amounts of PAN and $LiClO_4$, room temperature conductivity increased over four orders of magnitude from 10^{-10} to 10^{-6} Scm^{-1}. The temperature-dependent dc conductivity studies on PEO-PU/PAN/$LiClO_4$ semi-IPNs revealed a thermally activated ion transport process along with a Arrhenius to VTF type of transition around the melting temperature ($\sim$328 K) of poly (ethylene oxide) segments. To have a complete picture, it was felt necessary to characterize these semi-IPN systems for their thermo-mechanical stability. Results obtained from mechanical testing, DSC, DMTA and TGA for the PEO-PU/PAN semi-IPNs along with their $LiClO_4$ salt-complexes are presented in this paper.

Experimental

Materials

Castor oil (BSS Grade), Diphenylmethane diisocyanate (MDI) (Ind-ital Chem. Ltd.), Polyethylene glycol (PEG, MW = 4000), *N,N*-dimethylaniline (DMA) (SD Fine Chemicals), Acrylonitrile (SRL), Benzoyl peroxide and Tetrahydrofuran (THF) (Ranbaxy) were used as obtained. Lithium perchlorate trihydrate ($LiClO_4 \cdot 3H_2O$) was prepared by reacting purified Lithium carbonate (Li_2CO_3) with Perchloric acid ($HClO_4$). The product was then vacuum dried overnight at 90°C to obtain anhydrous $LiClO_4$ and stored in a desiccator under vacuum.

Synthesis

PEO-PU/PAN semi-IPNs were synthesized by simultaneous interpenetration of poly (acrylonitrile) (PAN) in the poly(ethylene oxide)-polyurethane (PEO-PU) network

through two mutually exclusive reactions, wherein an isocyanate terminated prepolymer was reacted with poly(ethylene glycol) to obtain the PEO-PU network along with free-radical polymerization of acrylonitrile. In a typical reaction, the isocyanate-terminated urethane prepolymer was synthesized by reacting castor oil with excess of MDI in THF for 1 h at room temperature under nitrogen atmosphere. The prepolymer was then mixed with PEG, the second monomer (acrylonitrile), benzoyl peroxide (initiator) and *N,N*-dimethylaniline (catalyst). The schematic pathways for the formation of the isocyanate- terminated prepolymer, poly(ethylene oxide)-polyurethane (PEO-PU) network and poly(acrylonitrile) (PAN) are shown in Schemes 1 and 2. The mixture was degassed and stirred under nitrogen atmosphere at room temperature for 30 min. The viscous solution was then cast in a Teflon mold. The curing was initially done at room temperature for 24 h and subsequently at 80°C in a vacuum oven for another 24 h to get the semi-IPN of PEO-PU/PAN. Semi-IPNs of different compositions having PEO-PU/PAN weight ratios 90/10, 80/20, 70/30, 60/40, 50/50, 40/60, and 30/70 and the parent system PEO-PU network (100/0) were synthesized and stored under vacuum. For the synthesis of the urethane networks the −OH/−NCO ratio of 1:1.25 was maintained with allowance for the presence of 0.01% moisture and the reaction was monitored by FT-IR (29).

Doping was achieved by simple dissolution of lithium perchlorate in the reaction mixture. PEO-PU/PAN/$LiClO_4$ doped semi-IPNs with EO/Li mole ratios of 100, 60, 30, 20, 15, 10 and 5 were thus synthesized where, EO represents the amount of ethylene oxide repeating units. The samples are coded in the order of the PEO-PU/PAN weight ratio followed by their respective EO/Li ratio (for example, 80/20/100 corresponds to a PEO-PU/PAN semi-IPN of weight ratio 80/20 doped with $LiClO_4$, with EO/Li ratio of 100).

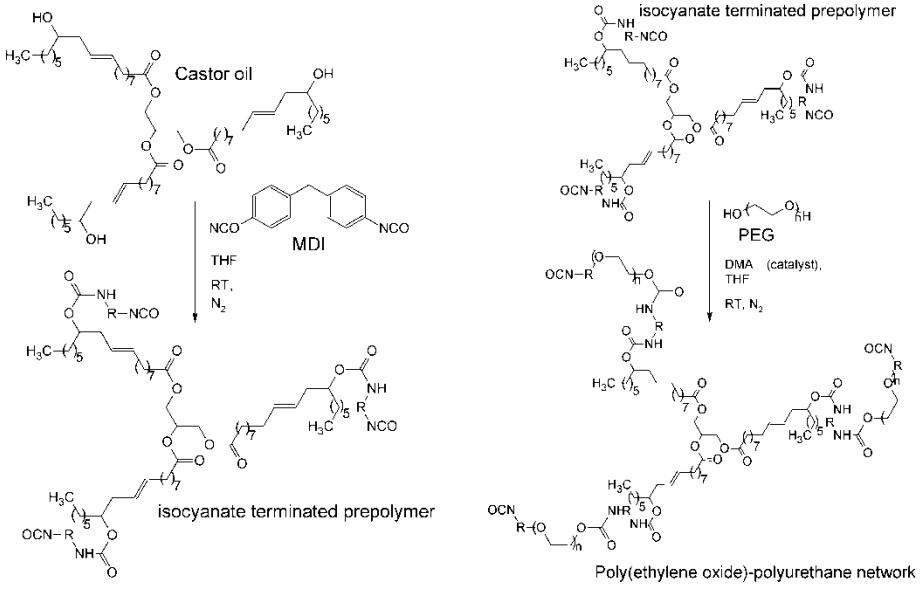

Scheme 1. Reaction pathways showing the formation of isocyanate terminated prepolymer from castor oil and diphenylmethane diisocyanate and the formation of poly(ethylene oxide)-polyurethane network from the isocyanate terminated prepolymer and poly(ethylene glycol).

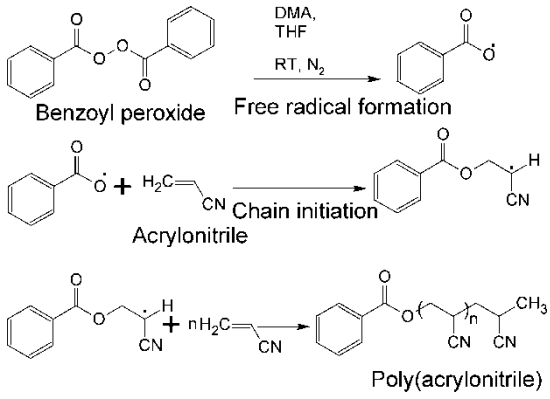

Scheme 2. Reaction pathway showing the formation of poly(acrylonitrile) by free radical polymerization of acrylonitrile using benzoyl peroxide.

Transmission Electron Microscopy

Transmission electron microscopy (TEM) studies of the semi-IPNs were carried out on a JEOL-JEM 100CX microscope. Films of $\sim 0.05\,\mu m$ thickness were solvent cast, lifted on copper grids and stained using osmium tetraoxide (OsO_4) prior to the analysis.

Differential Scanning Calorimetry

The thermal properties of the parent system (PEO-PU network), PEO-PU/PAN semi-IPNs and PEO-PU/PAN/$LiClO_4$ semi-IPN salt complexes have been investigated using a Differential Scanning Analyzer 2010 (TA Instruments). The samples, approximately of 10 mg, sealed in aluminum pans were quenched to $-130^{\circ}C$, and then heated at a scan rate of $10^{\circ}C\ min^{-1}$ under nitrogen atmosphere. The DSC thermograms were recorded in the range of $-120^{\circ}C$ to $150^{\circ}C$. The glass transition temperature (T_g), cold crystallization peak temperature (T_c), crystalline melting temperature (T_m), the corresponding enthalpy change (ΔH) associated with T_c and T_m and the percentage degree of crystallinity ($\chi\%$) were obtained using the thermal analysis software provided along with the instrument.

Thermogravimetric Analysis

Thermogravimetric analysis of the parent PEO-PU network, PEO-PU/PAN semi-IPNs and PEO-PU/PAN/$LiClO_4$ semi-IPN salt complexes were carried out using the Mettler Toledo TGA with star software. The samples ($\sim 5-10$ mg) were scanned in the temperature range $30-600^{\circ}C$ at a heating rate of $10^{\circ}C\ min^{-1}$ in air.

Tensile Measurements

Following ASTM D2370-1982 standards, the tensile properties of free standing films of the parent PEO-PU network, PEO-PU/PAN semi-IPNs and PEO-PU/PAN/$LiClO_4$ semi-IPN salt complexes were studied on a universal testing machine (UTM) AGS-10 k NG (Shimadzu). The measurements were carried out according to ASTM D-638 specifications, with a gauge length of 50 mm and crosshead a speed of 50 mm/min. The data reported is the average of three measurements.

Dynamic Mechanical Thermal Analysis

The viscoelastic or dynamic mechanical thermal properties of the undoped and $LiClO_4$ doped PEO-PU/PAN semi-IPN films were determined by using DMTA IV (Rheometric Scientific, UK). The samples of approximate size 10 mm × 10 mm × 0.8 mm were placed horizontally in a dual cantilever-bending beam clamping geometry. The storage modulus (E′), loss modulus (E″) and energy dissipation (tan δ) of the samples were measured in the temperature range of -120°C to 150°C at a frequency of 1 Hz, 0.003% minimum strain and at a heating ramp of 5°C min^{-1}.

Results and Discussion

Morphology

Two diffused regions were observed for the parent system 100/0 throughout the polymer matrix, as shown in the TEM micrographs (Figure 1). The darker regions are presumably due to the presence of semi-crystalline domains interspersed in the amorphous polymer matrix. In the case of a typical PEO-PU/PAN semi-IPN (60/40), two distinct phases were clearly observed where the poly(acrylonitrile) domains are seen as spheres of $\sim 50-200$ nm dispersed in the PEO-PU matrix. This morphology is typical for two component interpenetrating polymer networks, where one of the components undergoes nucleation and growth and is arrested at this stage due to gelation (30). Nevertheless, the electron microscopy studies showed beyond doubt that though the PEO-PU and PAN are not quite miscible the phase separation/segregation is confined to nanometer regime due to the formation of semi-interpenetrating polymer networks.

Differential Scanning Calorimetry

The effect of composition on the physical properties of the polymer materials can be best analyzed by studying the thermal characteristics. Differential scanning calorimetry (DSC) is an ideally suited probe to provide useful insights on the morphologically based thermal transitions in polymer matrices.

The glass transition temperature (T_g), the cold crystallization peak temperature (T_c) and the crystalline melting temperature (T_m) were determined from the DSC traces for

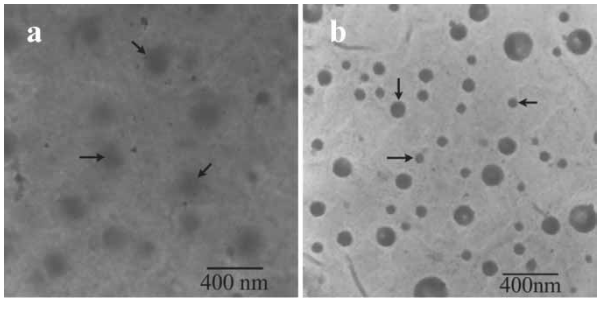

Figure 1. Transmission electron micrographs of (a) parent system PEO-PU network (100/0) and (b) PEO-PU/PAN semi-IPN (60/40) stained using OsO_4. The arrows in Figure (a) show the crystalline domains of PEO and in Figure (b) arrows show the poly(acrylonitrile) phase distributed in the poly(ethylene oxide)-polyurethane matrix.

the synthesized PEO-PU/PAN semi-IPNs. The apparent enthalpies of crystallization (ΔH_c) and melting (ΔH_m) are derived from the area under the exothermic (T_c) and endothermic (T_m) peaks, respectively. The degree of crystallinity (χ) of the PEO fraction in the matrix is calculated from the equation:

$$\chi = \Delta H_{m1}(PEO)/\Delta H_m^o(PEO). \quad (1)$$

where, ΔH_m^o (PEO) $= 205\,Jg^{-1}$ is the heat of melting per gram of 100% crystalline PEO and ΔH_{m1} (PEO) is the apparent enthalpy of melting per gram of the PEO (31). The values of T_g, T_c and T_m, along with the associated enthalpy (ΔH) change and degree of crystallinity (χ), as determined from the thermograms, are summarized in Table 1.

The T_g is a characteristic feature of the amorphous phase. For the parent PEO-PU network system the T_g was found to be at $\sim -44^\circ C$. In the semi-IPN systems the effect of poly(acrylonitrile) content on the PEO-PU network is observed as a variation of T_g compared to the parent system 100/0. With an increase in PAN content up to 20 wt% in the semi-IPNs, the T_g is first observed to decrease, further addition of PAN in the matrix led to a steady increase in T_g. The initial decrease in T_g observed due to addition of PAN could be attributed to the disruption of the ordered domains of the PEO. However, beyond 20 wt% PAN, the cumulative effect of crystallinity in both PEO and PAN results in a steady rise in T_g. Nevertheless, the glass transition temperature of all the semi-IPN compositions is found to be well below room temperature, which satisfies one of the major prerequisites of a polymer material to serve as a host matrix for SPEs (3–6).

Traditionally, the equations based on the free volume hypothesis have been used to model the compositional dependence and blend miscibility is often quantified by analyzing the compositional dependence of T_g (32–34). Thus, the T_g of synthesized PEO-PU/PAN semi-IPNs should ideally be a compromise between the T_g of PEO-PU network ($\sim -44^\circ C$) and that of PAN ($\sim 98^\circ C$) which can indicate the extent of miscibility between the two polymers. Even though, in the case of all the synthesized PEO-PU/PAN semi-IPN systems, the T_g is found to be in the range of $-50^\circ C$ to $-35^\circ C$, neither of the compositional dependence equations is found to hold good. Nevertheless, it is well known that a reasonably miscible interpenetrating polymer network could be formed from polymers that have completely immiscible linear chains (30). Hence, though PEO-PU and PAN are not quite compatible, because of the formation of the interpenetrating network, a forced miscibility between the two individual polymers has been achieved. This is also supported by the electron microscopy study, wherein it was observed that the phase separation/segregation is constrained within 50–200 nm.

All the semi-IPN compositions showed an exothermic peak corresponding to the cold crystallization transition temperature (T_c) and a sharp endothermic peak around 45–55°C, attributed to the melting temperature (T_m) of the crystalline domains in PEO. These transitions indicate the presence of a considerable amount of crystallinity (~ 10–15%) in the semi-IPNs.

Figure 2(A) and (B) shows the DSC thermograms for the parent system and a typical semi-IPN system (80/20) doped with $LiClO_4$. As compared to the undoped semi-IPN systems, the $LiClO_4$ doped parent system (100/0) and the semi-IPNs showed an initial decrease in the T_g from $-43.6^\circ C$ to $-48.6^\circ C$. Since salt solvation in such systems primarily occurs in the PEO rich phases (3–6), this decrease in the T_g with the initial addition of $LiClO_4$ in the semi-IPN system was attributed to the disruption of the ordered crystalline domains in the PEO rich phase. However, the Tg increased steadily with a further increase in the $LiClO_4$ concentration, suggesting a progressive decrease

Table 1
Effect of PAN and $LiClO_4$ concentration on the glass transition temperature (T_g), cold crystallization temperature (T_c), crystalline melting temperature (T_m), enthalpy change (ΔH) and degree of crystallinity (χ) of the PEO-PU/PAN semi-IPNs

Semi-IPN composition	T_g (°C)	T_c (°C)	T_m (°C)	$-\Delta H_c$ (Jg^{-1})	$-\Delta H_m$ (Jg^{-1})	χ^a (%)
100/0	−43.6	−2.6	40.8	15.4	23.2	11.3
90/10	−45.0	−5.4	40.1	16.2	25.4	12.4
80/20	−47.9	−1.4	40.5	12.4	16.9	8.2
70/30	−46.9	−5.8	42.2	16.7	26.9	13.1
60/40	−44.1	−11.2	44.9	19.8	39.4	19.2
50/50	−41.7	7.5	55.5	0.8	24.4	11.9
40/60	−38.5	**	56.1	**	27.3	13.3
100/0/100	−48.6	2.4	43.9	15.3	24.6	12.0
100/0/60	−44.9	11.2	44.3	8.6	13.4	6.5
100/0/30	−42.7	17.4	45.6	9.2	12.9	6.3
100/0/20	−41.9	−4.0	40.9	4.4	8.9	4.3
100/0/15	−40.8	−2.4	44.3	2.8	6.3	3.1
100/0/10	−39.3	20.3	48.7	2.1	4.2	2.0
100/0/5	−37.6	23.1	52.6	1.3	1.7	0.8
80/20/100	−48.1	4.2	43.8	26.1	35.1	17.1
80/20/60	−43.6	15.8	38.8	2.1	3.4	1.7
80/20/30	−40.9	28.0	52.2	0.8	1.2	0.5
80/20/20	−39.8	**	**	**	**	**
80/20/15	−38.1	**	**	**	**	**
80/20/10	−34.0	**	**	**	**	**
80/20/5	−32.6	**	**	**	**	**
60/40/100	−46.9	1.3	46.6	21.7	31.7	15.5
60/40/60	−43.1	11.6	45.7	18.5	23.2	11.3
60/40/30	−38.4	**	55.1	**	2.8	1.4
60/40/20	−35.3	**	**	**	**	**
60/40/15	−32.6	**	**	**	**	**
60/40/10	−29.3	**	**	**	**	**
60/40/5	−26.8	**	**	**	**	**

*Absence of T_c, T_m peaks in the DSC thermograms.
[a]Normalized values to 100% PEO.
The samples are coded in the order of the PEO-PU/PAN weight ratio followed by their respective EO/Li mole ratio.

in the segmental mobility of the polymer chains. The latter is attributed to the formation of Li^+-ion mediated pseudo-crosslinks within the polymer matrix (35).

In the parent (100/0) system, the T_c and T_m peaks were observed throughout the salt concentrations studied with the peaks showing a marked decrease, suggesting a reduction in the degree of crystallinity with increasing salt concentration. However, in the thermogram traces for the doped semi-IPNs, complete disappearance of both T_c and T_m peaks were observed with increasing concentration of $LiClO_4$. The large T_c and T_m peaks for the semi-IPNs with EO/Li mole ratios 100, 60, and 30 indicate the presence of a

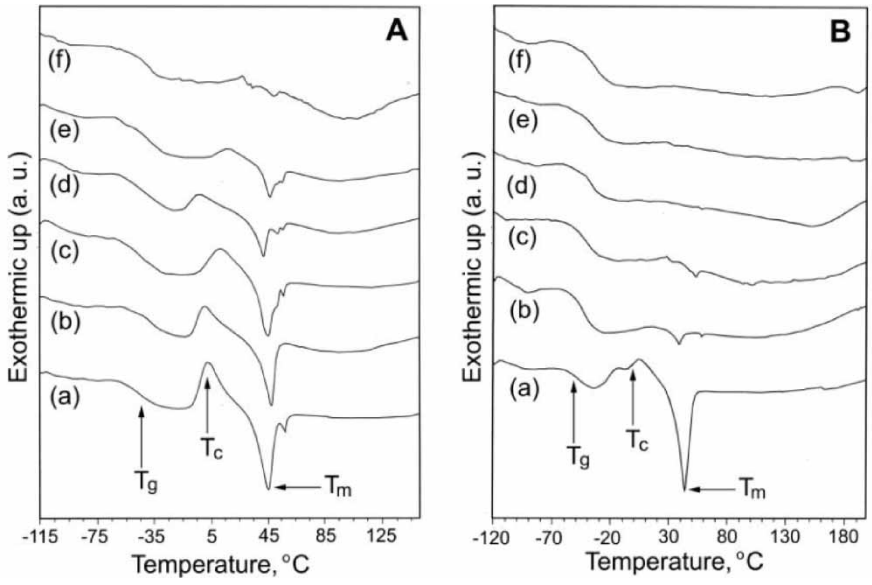

Figure 2. DSC thermograms of (A) parent system PEO-PU network (100/0) and (B) PEO-PU/PAN semi-IPNs 80/20 doped with $LiClO_4$. (a) EO/Li = 100, (b) EO/Li = 60, (c) EO/Li = 30, (d) EO/Li = 20, (e) EO/Li = 10, and (f) EO/Li = 5.

considerable amount of crystalline domains at room temperature. However, semi-IPNs with EO/Li ratios below 30 are found to be amorphous. This signifies a complete transformation in morphology of PEO from semicrystalline to an amorphous phase above a critical $LiClO_4$ concentration. It can, therefore, be inferred that during the curing step of the semi-IPNs, ordering and formation of crystalline domains is prevented by the considerable increase in the number of pseudo-crosslinks. Thus, at higher concentrations of $LiClO_4$, two opposing factors operate simultaneously within the semi-IPNs. Though the Li^+-ions act as transient crosslinkers resulting in the progressive immobilization of the polymer chain segments leading to the rise in T_g, the same feature helps in reducing the degree of crystallinity.

Similar trends were observed for all the PEO-PU/PAN semi-IPN compositions doped with $LiClO_4$. As seen from the calculated data listed in Table 1, the degree of crystallinity reduces dramatically with increasing salt concentration; and for EO/Li ratios <30 the semi-IPN matrix is found to be completely amorphous. Interestingly, even at 200°C, no degradation of the polymer matrix is observed in the DSC traces. This signifies that the synthesized semi-IPNs are thermally quite stable and are suitable for use in the desired application as electrolytes in rechargeable batteries at ambient operating conditions.

Thermogravimetric Analysis

The thermal stability and thermal decomposition behavior for the PEO-PU/PAN semi-IPNs were further investigated using thermogravimetric analysis (TGA). The TGA plots in Figure 3(A) reveals that heating the polymer in the range of 30–150°C results in a minimal weight loss of 1–3%. The small weight losses observed in the initial stages are presumably caused by the evaporation of low molecular weight components as well as moisture present in the polymers. In the temperature range 200–550°C, the TG plots

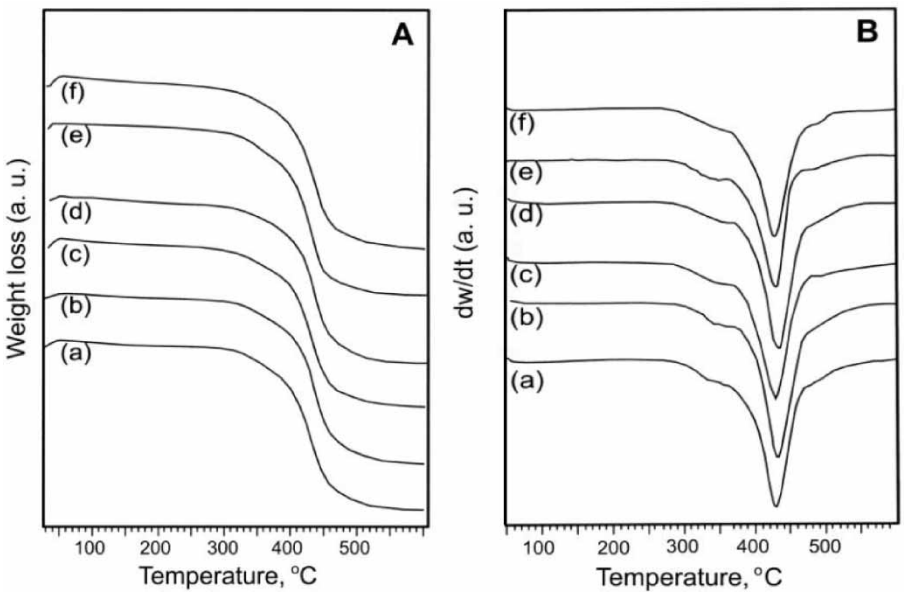

Figure 3. A) Thermogravimetric profiles of (a) parent system PEO-PU network (100/0) and PEO-PU/PAN semi-IPNs (b) 90/10, (c) 80/20, (d) 70/30, (e) 60/40, (f) 50/50, and (B) their respective differential thermogravimetric profiles.

of the semi-IPNs shows a typical sigmoidal form and exhibits three decomposition stages as revealed in the DTA plots (Figure 3(B)).

The TGA and DTA plots for the composition range of the semi-IPNs exhibit little difference in their thermal degradation profile, compared to the 100/0 parent system. This suggests that the thermal decomposition behavior of the PEO-PU/PAN semi-IPNs is independent of the PAN content in the polymer matrix. This observation may be attributed to the oxidative stabilization of PAN, which transforms to a highly crosslinked cyclized structure when heated beyond 200°C. The three-stage process for the thermal-oxidative degradation reflects the soft and hard segment degradation of the PEO-PU network (36–39). The degradation onset temperature (T_0) was around 240°C (start of the first stage), due to the thermal destruction of the urethane groups in the network. An increasing decomposition rate being observed between 380–470°C with the weight loss of about 70–80 wt% (the second stage), can be attributed to the polyethylene oxide chain scission with maximum rate of weight loss at 430°C. The third stage for the temperatures beyond 470°C corresponds to the advanced fragmentation of the chains formed in the first and the second stages of decomposition, as well as to the secondary reactions of dehydrogenation and gasification processes.

The TG and DTA profiles for the typical semi-IPN system (60/40) doped with different concentrations of $LiClO_4$ are shown in Figure 4(A) and (B). The decomposition behavior remains almost similar except that the rate of decomposition in the first stage, with a maximum weight loss around 330°C, shows a steady increase in the rate with increase in salt concentration in the system. This may be attributed to the scission of the Li^+-ion mediated pseudo-crosslinks along with the destruction of the urethane linkages. Nevertheless, the negligible weight loss of the salt incorporated polymer

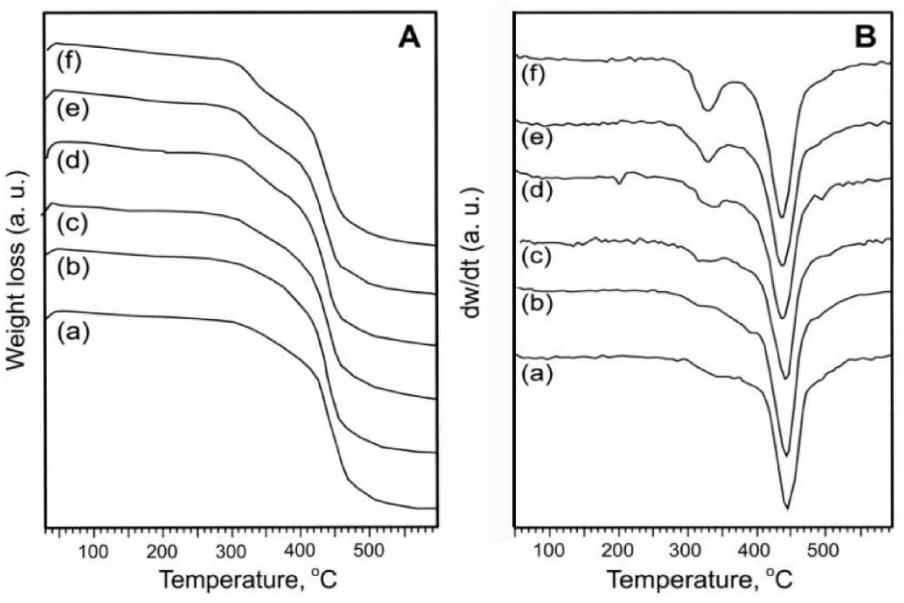

Figure 4. A) Thermogravimetric profiles of PEO-PU/PAN semi-IPN 60/40 doped with $LiClO_4$ (a) EO/Li = 100, (b) EO/Li = 60, (c) EO/Li = 30, (d) EO/Li = 20, (e) EO/Li = 10, and (f) EO/Li = 5 and (B) their respective differential thermogravimetric profiles.

matrix, even at 200°C, signifies that the synthesized semi-IPNs are thermally quite stable and can be used for the desired application at ambient operating conditions.

Tensile Properties

The synthesized PEO-PU/PAN semi-IPNs were tested for their dimensional and mechanical properties to reveal the effect of PAN and $LiClO_4$ content. The stress-strain data obtained from tensile studies provided information on the strength, modulus and elongation of the parent system (100/0) and the semi-IPNs, as listed in Table 2. The data reported is the average of three measurements and the maximum error associated with the determination of the yield stress, yield strain, elastic modulus, ultimate tensile strength, and % elongation are within the confidence limit of $\pm$ 10%.

When compared to the parent 100/0 system, the tensile strength and elastic modulus of the semi-IPNs is seen to increase steadily with an increase in the PAN content. The modulus of resilience, which is the capacity of a material to absorb energy while deformed elastically in the elastic region, is also seen to increase steadily with incorporation of PAN. The rigidity of PAN is therefore the dominant factor that determines the materials' ultimate tensile strength and modulus. The ultimate elongation measured from the strain value at break point taken as the index of flexibility though does not alter much with the incorporation of PAN. The elastic property thus remains much less sensitive to the PAN content. However, stresses between 1–4 MPa and elongation at break value (strain) $\sim$55% are indicative of their good mechanical strength. It can, hence, be deduced that PAN does not alter the flexibility while improving the strength of the parent system.

Table 2
Effect of PAN and $LiClO_4$ concentration on the yield stress (σ_y), yield strain (ε_y), elastic modulus (Y), ultimate tensile strength (σ_{max}), ultimate elongation and modulus of resilience (U_r) of the PEO-PU/PAN semi-IPNs

Semi-IPN Composition	$\sigma_y \pm 0.05$ (MPa)	$\varepsilon_y \pm 0.5$ (%)	$Y \pm 1.0$ (MPa)	$\sigma_{max} \pm 0.1$ (MPa)	(%) $\pm$ 10 elongation	U_r (MPa)
100/0	0.14	6.6	2.1	1.16	59.5	4.6×10^{-3}
90/10	0.19	4.4	4.8	1.24	53.4	4.2×10^{-3}
80/20	0.25	4.8	5.2	1.32	56.2	6.0×10^{-3}
70/30	0.36	5.5	6.6	1.45	45.4	9.9×10^{-3}
60/40	0.86	8.8	9.8	2.42	55.7	3.8×10^{-2}
50/50	1.51	8.8	17.2	2.87	52.2	6.6×10^{-2}
40/60	1.95	8.2	23.8	3.38	54.3	8.0×10^{-2}
60/40/100	0.95	9.9	9.5	2.28	51.8	4.7×10^{-2}
60/40/60	0.75	8.0	9.3	2.07	48.1	3.0×10^{-2}
60/40/30	0.53	5.9	8.9	1.62	43.8	1.6×10^{-2}
60/40/20	0.29	5.9	4.9	0.97	43.6	8.7×10^{-3}
60/40/15	0.11	4.8	2.3	0.54	41.6	2.6×10^{-3}
60/40/10	0.06	4.1	1.5	0.53	41.3	1.2×10^{-3}

The samples are coded in the order of the PEO-PU/PAN weight ratio followed by their respective EO/Li mole ratio.

With an increase in the $LiClO_4$ content in the semi-IPN, a steady decrease was observed in the tensile strength, elastic modulus, elongation at break and modulus of resilience. The decrease in the tensile strength and modulus of the semi-IPNs indicates a progressive decrease in the degree of crystallinity in the bulk with an increase in salt concentration. The increase in the number of transient crosslinks due to Li^+-ions in the system however affects the flexibility of the semi-IPNs adversely. This is manifested by a slight decrease in the ultimate elongation with an increase in $LiClO_4$ content. The data obtained from DSC studies, as explained in the previous section, lends further credence to these observations.

Dynamic Mechanical Thermal Behavior

The dynamic mechanical technique of impressing a small oscillating mechanical strain on a solid or viscoelastic liquid and resolving the stress into real and imaginary components, detects essentially all changes in the state of molecular motion as the temperature is varied (39). In solid elastomers, the ability of the material to damp vibration through intrinsic absorption depends on Young's modulus and is characterized in dynamic mechanical terms as a complex modulus (E^*) expressed as follows:

$$E^* = E' - iE''. \tag{2}$$

The storage modulus (E') and loss modulus (E'') are the quantities of energy stored through elastic behavior and energy lost through conversion to heat via molecular friction, respectively. When a polymer is in its viscoelastic region, which is the transition from a hard glassy state to the soft rubbery state, it exhibits the highest level of damping.

The peak obtained in the DMTA traces for either the loss modulus (E″) or loss tangent (tan $\delta = E''/E'$) are hence used to determine the T_g. The damping peak is associated with the partial loosening of the polymer structure so that groups and small chain segments can move. This occurs near T_g at low frequencies. The tanδ peak at a frequency of one cycle per second generally is at a temperature 5°C to 15°C above the T_g as measured by other techniques like DSC or DTA (39). The maximum in the loss modulus (E″) at low frequencies is however very close to T_g.

Figure 5(a)–(d) shows the DMTA traces for the parent system (100/0), PEO-PU/PAN semi-IPN (60/40) and the $LiClO_4$ doped semi-IPN (60/40/30, 60/40/10). For all the PEO-PU/PAN semi-IPNs, the tan δ peak was found to be broad and showed considerable shift from the T_g, whereas the temperature corresponding to E″ peak was very close to T_g, as obtained from DSC (Table 3). The T_g for the semi-IPNs showed a steady increase with the increase in PAN and $LiClO_4$ content. The room temperature storage modulus (E′) was found comparable to the values for the elastic modulus (Y) in the tensile studies (Table 2). The E″ was found to increase with increase in PAN content and decrease with the increase in $LiClO_4$ concentration. The results obtained and the trends observed were in good agreement with the DSC and tensile studies.

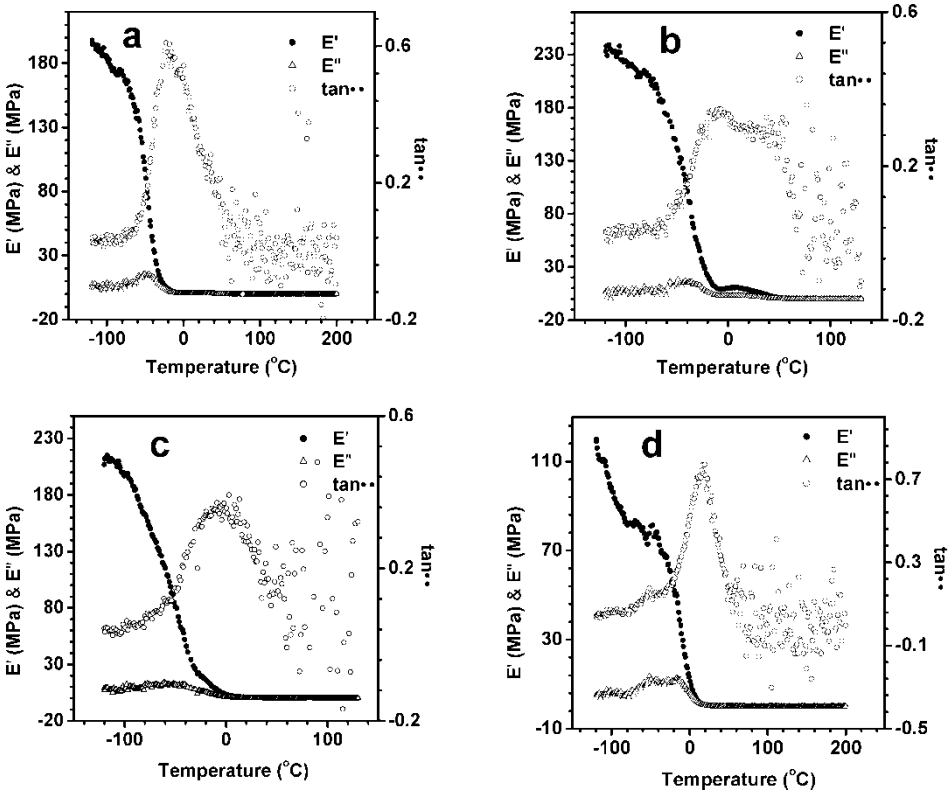

Figure 5. DMTA profiles of (a) parent system PEO-PU network (100/0), (b) PEO-PU/PAN semi-IPN (60/40), (c) PEO-PU/PAN/$LiClO_4$ semi-IPN 60/40/30, and (d) PEO-PU/PAN/$LiClO_4$ semi-IPN 60/40/10.

Table 3
Effect of PAN and $LiClO_4$ concentration on the peak temperatures of loss modulus (E″) and tan δ along with storage modulus (E′) obtained at 30°C and 80°C from the DMTA profiles

Semi-IPN composition	E″ (°C)	tanδ (°C)	E′(MPa) (30°C)	E′(MPa) (80°C)
100/0	−50.3	−22.6	1.12	0.065
80/20	−45.0	−11.4	4.15	0.11
60/40	−41.8	−8.3	6.1	0.08
60/40/100	−60.6	4.2	1.41	0.05
60/40/30	−52.0	8	0.54	0.02
60/40/10	−16.2	16.9	0.25	0.04

The samples are coded in the order of the PEO-PU/PAN weight ratio followed by their respective EO/Li mole ratio.

Conclusions

A detailed investigation on the thermo-mechanical properties of PEO-PU/PAN semi-IPNs along with their $LiClO_4$ salt complexes was carried out. The T_g of all the compositions of undoped and doped semi-IPNs, obtained by DSC, remained well below room temperature, satisfying one of the essential properties to serve as a SPE host matrix. The crystallization process in the PEO segments of the PEO-PU/PAN semi-IPNs was prevented at higher salt concentration, which is attributed to the Li^+ ion mediated pseudo-crosslinks. The semi-IPNs showed good thermal stability with a three-stage degradation process, which is independent of the PAN content as observed by DTA. The incorporation of PAN in the PEO-PU networks results in improved mechanical properties such as tensile strength and modulus while retaining the flexibility of the semi-IPNs. The DMTA results further support the observations of DSC and tensile measurements.

In summary, a series of PEO-PU/PAN/$LiClO_4$ semi-IPN salt complexes with good mechanical, thermal and dimensional stability, along with low T_g and degree of crystallinity have been achieved, which satisfies all the prerequisites of being a promising solid polymer electrolyte.

Acknowledgements

PB gratefully acknowledges 'Council of Scientific and Industrial Research', India for the financial assistance in the form of a senior research fellowship (SRF).

References

1. Fenton, D.E., Parker, J.M., and Wright, P.V. (1973) *Polymer*, 14 (11): 589.
2. Armand, M.B., Chabagno, J.M., and Duclot, M.J. (1979) Polyethers as Solid Electrolytes. In *Fast Ion Transport in Solids Electrodes Electrolytes, Proc. Int. Conf.*; Vashishta, P., Mundy, J.N. and Shenoy, G.K., Eds.; Elsevier North: Amsterdam, Holland; Vol. 131.
3. Gray, F.M. (1991) In *Solid Polymer Electrolytes-Fundamentals and Technological Applications*; VCH: Weinhem, Germany.
4. MacCallum, J.R. and Vincent, C.A. (1987) *Polymer Electrolyte Reviews-1*; MacCallum, J.R. and Vincent, C.A., Eds.; Elsevier Applied Science: New York; Vol. 1.

5. Ratner, M.A. and Shriver, D.F. (1988) *Chem. Rev.*, 88 (1): 109–124.
6. Armand, M. (1986) *Annu. Rev. Mater. Sci.*, 16: 245–261.
7. Eisenberg, A., Ovans, K., and Yoon, H.N. (1980) The Viscosity Enhancement of Polyethers by Salts. In *Ions in Polymers*; Eisenberg, A., Ed.; Advances in Chemistry Series 187, American Chemical Society: Washington, DC.
8. Cowie, J.M.G. and Cree, S.H. (1989) *Annu. Rev. Phys. Chem.*, 40: 85–113.
9. Druger, S.D., Nitzan, A., and Ratner, M. (1983) *J. Chem. Phys.*, 79 (6): 3133–3142.
10. Shi, J. and Vincent, C.A. (1993) *Solid State Ionics*, 60 (1–3): 11–17.
11. Gauthier, M., Fauteux, D., Vassort, G., Belanger, A., Duval, M., Ricous, P., Chabagno, J.M., Muller, D., Rigaud, M.B., Armand, M.B., and Deroo, D. (1985) *J. Electrochem. Soc.*, 132 (6): 1333–1340.
12. Abraham, K.M., Alamgir, M., and Perrotti, S.J. (1988) *J. Electrochem. Soc.*, 135 (2): 535–536.
13. Vallee, A., Besner, S., and Prud'Homme, J. (1992) *Electrochim Acta.*, 37 (9): 1579–1583.
14. Abraham, K.M. and Alamgir, M. (1990) *J. Electrochem. Soc.*, 136 (5): 1657–1658.
15. Perera, K., Dissanayake, M.A.K.L., and Bandaranayake, P.W.S.K. (2000) *Electrochim. Acta.*, 45 (8): 1361–1369.
16. Watanabe, M., Kanba, M., Nagaoka, K., and Shinohara, I. (1983) *J. Polym. Sci.*, 21 (6): 939–948.
17. Rajendran, S., Mahalingam, T., and Kannan, R. (2000) *Solid State Ionics*, 130 (1): 143–148.
18. Forsyth, M., Jiazeng, S., and MacFarlan, D.R. (2000) *Electrochim. Acta*, 45 (8): 1249–1254.
19. Li, J., Pratt, L.M., and Khan, I.M. (1995) *J. Polym Sci. Polym. Chem.*, 33 (10): 1657–1663.
20. Acosta, J.L. and Morales, E. (1996) *J. Appl. Polym. Sci.*, 60 (8): 1185–1191.
21. Kobayashi, N., Uchiyama, M., Shigehara, K., and Tsuchida, E. (1985) *J. Phys. Chem.*, 89 (6): 987–991.
22. Robitaille, C. and Prud'homme, J. (1983) *Macromolecules*, 16 (4): 665–671.
23. Watanabe, M., Sanui, K., Ogata, N., Kobayashi, T., and Ohtaki, Z. (1985) *J. Appl. Phys.*, 57 (1): 123–128.
24. Florjanczyk, Z., Krawiec, W., Wieczorek, W., and Siekierski, M. (1995) *J. Polym. Sci. Polym. Phys.*, 33 (4): 629–636.
25. Allcock, H.R., O'Connor, S.J.M., Olmeijer, D.L., Napierala, M.E., and Cameron, C.G. (1996) *Macromolecules*, 29 (23): 7544–7552.
26. Leveque, M., Le Nest, J.F., Gandini, A., and Cheradame, H. (1983) *Makromol. Chem. Rapid Commun.*, 4 (7): 497–502.
27. Zhang, Z. and Fang, S.J. (2000) *Appl. Polym. Sci.*, 77 (13): 2957–2962.
28. Ichikawa, K., Dickinson, L.C., MacKnight, W.J., Watanabe, M., and Ogata, N. (1992) *Polymer*, 33 (22): 4699–4704.
29. Basak, P. and Manorama, S.V. (2004) *Solid State Ionics*, 167 (1–2): 113–121.
30. Sperling, L.H. (1994) Interpenetrating Polymer Networks: An Overview. In *Interpenetrating Polymer Networks*; Klempner, D., Sperling, L.H. and Utracki, L.A., Eds.; Advances in Chemistry Series, ACS: Washington, DC; Vol. 239, 3–38.
31. Cosaert, K., Eeckhout, E., Goethals, E., Prez, F.D., Guegan, P., and Cheradame, H. (2002) *Polym. Int.*, 51 (11): 1231–1237.
32. Fox, T.G. (1956) *Bull. Am. Phys. Soc.*, 1 (2): 123.
33. Gordon, M. and Taylor, J.S. (1952) *J. Appl. Chem.*, 2: 493–500.
34. Wood, L.A. (1958) *J. Polym. Sci.*, 28: 319–330.
35. Albinsson, I., Mellander, B.–E., and Stevens, J.R. (1992) *J. Chem. Phys.*, 96 (1): 681–690.
36. Kim, S.J., Park, S.J., Kim, I.Y., Chung, T.D., Kim, H.C., and Kim, S.I. (2003) *J. Appl. Polym. Sci.*, 90 (3): 881–885.
37. Cascaval, C.N., Rosu, D., Rosu, L., and Ciobanu, C. (2003) *Polym. Test.*, 22 (1): 45–49.
38. Fainleib, A., Kozak, N., Grigoryeva, O., Nizelskii, Y., Grytsenko, V., Pissis, P., and Boiteux, G. (2002) *Polym. Deg. Stab.*, 76 (3): 393–399.
39. Nielsen, L.E. (1974) Mechanical Properties of Polymers and Composites. Marcel Dekker Inc.: NY; Vol. 1.